PHYSICAL REVIEW D **94,** 044046 (2016)

Dynamics of gravitating hadron matter in a Bianchi-IX cosmological model

Sergey A. Pavluchenko
Programa de Pós-Graduação em Física, Universidade Federal do Maranhão (UFMA), 65085-580 São Luís, Maranhão, Brazil
(Received 5 July 2016; published 24 August 2016)

We perform an analysis of the Einstein-Skyrme cosmological model in the Bianchi-IX background. We analytically describe asymptotic regimes and semianalytically describe generic regimes. It appears that depending on the product of the Newtonian constant κ with Skyrme coupling K, in the absence of the cosmological term, there are three possible regimes: recollapse with $\kappa K < 2$ and two power-law regimes, $\propto t^{1/2}$ for $\kappa K = 2$ and $\propto t$ for $\kappa K > 2$. In the presence of the positive cosmological term, power-law regimes turn to the exponential (de Sitter) ones, while the recollapse regime turns to the exponential if the value for the Λ-term is sufficiently large, otherwise the regime remains recollapse. The negative cosmological term leads to the recollapse regardless of κK. All nonsingular regimes have the squashing coefficient $a(t) \to 1$ at late times, which is associated with restoring symmetry dynamics. Also all nonsingular regimes appear to be linearly stable exponential solutions always, while power-law regimes for an open region of the initial conditions.

DOI: 10.1103/PhysRevD.94.044046

I. INTRODUCTION

One of the most important nonlinear field theories is the sigma model, with its applications covering many aspects of quantum physics (see, e.g., [1] for review), but within this model, it is impossible to build static soliton solutions in $3 + 1$ dimensions. To overcome this, Skyrme introduced [2] a term, which allows static soliton solutions with finite energy, called Skyrmions (see also [1,3] for review) to exist. It appears that excitations around Skyrme solutions may represent fermionic degrees of freedom, suitable to describe baryons (see [4] for detailed calculations and [5–8] for examples). The winding number of Skyrmions is identified with the baryon number in particle physics [9]. Apart from particle and nuclear physics, Skyrme theory is relevant to astrophysics [10], Bose-Einstein condensates [11], nematic liquids [12], magnetic structures [13], and condensed matter physics [14]. Also, Skyrme theory naturally appears in AdS/CFT context [15].

Due to the highly nonlinear character of sigma and Skyrme models, it is very difficult to build exact solutions in both of them. So, to make field equations more tractable, one usually adopts certain *ansatz*. For the Skyrme model, one of the best known and mostly used is the hedgehog *ansatz* for spherically symmetric systems, which reduces field equations to a single scalar equation. It is worth mentioning that recently this *ansatz* was generalized [16] for nonspherically-symmetric cases.

Use of the hedgehog *ansatz* allows study of self-gravitating Skyrme models. In particular, the potential presence of Skyrme hair for spherically symmetric black hole configurations [17] was demonstrated. This is the first genuine counterexample to "no hair" conjecture, which appears to be stable [18]; its particle-like [19] counterparts and dynamical configurations [20] have been studied numerically. After that, more realistic spherically and axially symmetric black hole and regular configurations were studied [21].

Apart from spherically symmetric configurations, of particular interest are cosmological-type solutions. The generalized hedgehog *ansatz* makes it possible to write down simplified field equations for nonspherically symmetric configurations, which we used to perform analysis of Bianchi-I and Kantowski-Sachs models for Einstein-Skyrme cosmology with the Λ-term [22] (a particular subcase was studied in [23]). The paper [24] was a logical continuation of them, as the particular solution of the Bianchi-IX cosmological model was described. The analysis suggests that, based on the static counterpart of this model, the construction of exact multi-Skyrmion configurations composed by elementary spherically symmetric Skyrmions with a nontrivial winding number in four dimensions is possible [25] (see also [26] for possible generalization to higher $SU(N)$ models).

In this paper, we consider the full Bianchi-IX cosmological model in the Einstein-Skyrme system. Our study is motivated from both the field theory and cosmological point of view. Indeed, this is one of the few (if not the only) system where one can study analytically dynamical and cosmological consequences of the conserved topological charge, which in this particular case is associated with the baryon number. From the cosmological point of view, the Bianchi-IX model is well known and well studied in cosmology, for instance, for the proof of inevitability of the physical singularity through the oscillatory approach to it [27]. So, if we consider the Bianchi-IX model, the results

could be translated and compared with the counterparts from our physical Universe.

The structure of the manuscript is as follows: First, we review the Einstein-Skyrme system and derive basic equations, and then, we study the asymptotic case both with and without the Λ-term. After that, we study the general case, address linear stability of the obtained solutions, and finally, discuss and summarize the results.

II. EQUATIONS OF MOTION

The Skyrme action can be constructed in the following way: Let U be an $SU(2)$ valued scalar field. We can then define the quantities

$$A^i_\mu t_i \equiv A_\mu = U^{-1}\nabla_\mu U,$$

$$F_{\mu\nu} = [A_\mu, A_\nu].$$

Here, the Latin indices correspond to the group indices, and the generators t_i of $SU(2)$ are related to the Pauli matrices by $t_i = -i\sigma_i$. The Skyrme action is then defined as

$$S_{\text{Skyrme}} = \frac{K}{2}\int d^4x\sqrt{-g}\text{Tr}\left(\frac{1}{2}A_\mu A^\mu + \frac{\lambda}{16}F_{\mu\nu}F^{\mu\nu}\right). \quad (1)$$

The case when $\lambda = 0$ is called the nonlinear sigma model, and the term which multiplies λ is called the Skyrme term. The total action for a self-gravitating Skyrme field reads

$$S = \int d^4x\sqrt{-g}\frac{R-2\Lambda}{2\kappa} + S_{\text{Skyrme}}, \quad (2)$$

where κ is the gravitational constant, R is the Ricci scalar, and Λ is the cosmological constant. The Skyrme field equation reads

$$\nabla^\mu A_\mu + \frac{\lambda}{4}\nabla^\mu[A^\nu, F_{\mu\nu}] = 0. \quad (3)$$

The topological charge of the Skyrme model is

$$w = -\frac{1}{24\pi^2}\int\limits_{t=\text{const}} \text{Tr}[\epsilon^{ijk}A_iA_jA_k], \quad (4)$$

and physically, it represents the baryonic charge.

The $SU(2)$ valued scalar field can be parametrized in a standard way,

$$U = \mathbf{I}Y^0 + Y^i t_i; \qquad U^{-1} = \mathbf{I}Y^0 - Y^i t_i,$$

where $Y^0 = Y^0(x^\mu)$ and $Y^i = Y^i(x^\mu)$ must satisfy $(Y^0)^2 + Y_iY^i = 1$. The most famous and most studied *ansatz* for searching solutions to the (nonself-gravitating) Skyrme theory is the so called "hedgehog," which is obtained by choosing

$$Y^0 = \cos(\alpha); \qquad Y^i = n^i\sin(\alpha),$$

where α is a radial profile function and n^i is a normal radial vector

$$n^1 = \sin\Theta\cos\Phi; \qquad n^2 = \sin\Theta\sin\Phi; \qquad n^3 = \cos\Theta.$$

As mentioned, we work with the Bianchi-IX metric,

$$ds^2 = -dt^2 + \frac{\rho^2(t)}{4} \times [a^2(t)(d\gamma + \cos\theta d\varphi)^2 + d\theta^2 + \sin^2\theta d\varphi^2], \quad (5)$$

where $\rho(t)$ is a global scale factor and $a(t)$ is a squashing coefficient. One can check that (see also [24]) with unit baryonic charge $w = +1$ (4), the configuration

$$\Phi = \frac{\gamma+\varphi}{2}, \quad \tan\Theta = \frac{\cot(\frac{\theta}{2})}{\cos(\frac{\gamma-\varphi}{2})}, \quad \tan\alpha = \frac{\sqrt{1+\tan^2\Theta}}{\tan(\frac{\gamma-\varphi}{2})} \quad (6)$$

identically satisfies the Skyrme field equations (3) on any background metric of the form (5). Now substituting metric (5) and configuration (6) into action (1) and (2), as well as into the hedgehog *ansatz*, one can derive equations of motion in the following form (see also [24]):

$$\begin{aligned}
&2a\rho^2(2\rho\dot{a} + 3a\dot{\rho})\dot{\rho} - 2a^2\rho^2(\Lambda\rho^2 + a^2 - 4) - \kappa K[(2\rho^2+\lambda)a^2 + \rho^2 + 2\lambda] = 0,\\
&2a^2\rho^2(2\rho\ddot{\rho} + \dot{\rho}^2) - 2a^2\rho^2(\Lambda\rho^2 + 3a^2 - 4) - \kappa K[(2\rho^2+\lambda)a^2 - \rho^2 - 2\lambda] = 0,\\
&a\rho^3(\rho\ddot{a} + 3\dot{\rho}\,\dot{a}) + (a^2-1)[\kappa K(\lambda+\rho^2) + 4a^2\rho^2] = 0.
\end{aligned} \quad (7)$$

III. ASYMPTOTIC $a(t) \equiv 1$ CASE

We start from the equations for the special case $a(t) \equiv 1$ after substituting it into (7):

$$\dot{\rho}^2 = \frac{\Lambda}{3}\rho^2 + \frac{\lambda\kappa K}{2\rho^2} + \frac{\kappa K - 2}{2}, \qquad \ddot{\rho} = \frac{\Lambda}{3}\rho - \frac{\lambda\kappa K}{2\rho^3}. \quad (8)$$

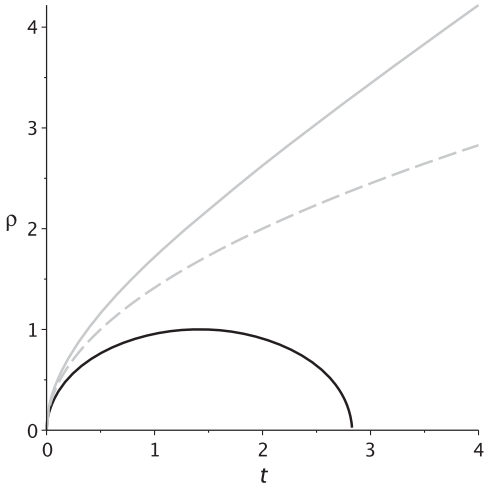

FIG. 1. Solutions of the $a(t) \equiv 1$ and $\Lambda = 0$ case: $\kappa K < 2$ in black, $\kappa K = 2$ in dashed gray, and $\kappa K > 2$ in solid gray (see the text for more details).

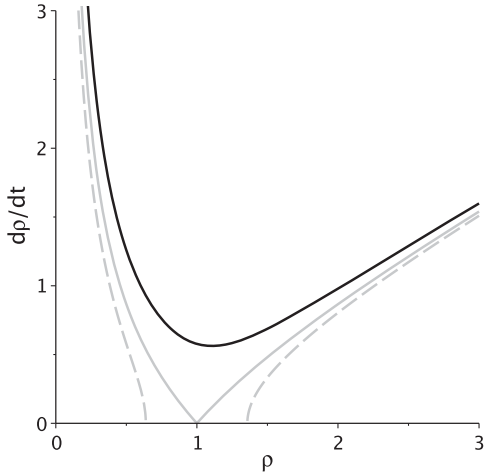

FIG. 2. Phase portrait of the $a(t) \equiv 1$ model with $\kappa K < 2$ and $\Lambda > 0$: cases with positive discriminant of (8) (black curve), zeroth (solid gray), and negative (dashed gray) (see the text for more details).

Let us first analyze the $\Lambda = 0$ case. In that case system, (8) has the exact solution with the integration constant which we fix from the condition $\rho \to 0$ as $t \to 0$; the resulting solution is

$$\rho = \tfrac{1}{\sqrt{2}} \sqrt{t((\kappa K - 2)t + 2\sqrt{2\lambda\kappa K})}. \tag{9}$$

One can see that for $\kappa K > 2$, the late-time asymptote is $\rho \propto t$, while the $\kappa K = 2$ solution (9) reduces to

$$\rho = \sqrt{2\sqrt{2}\lambda t}, \tag{10}$$

and one can see that its late-time asymptote is $\rho \propto t^{1/2}$. Finally, for $\kappa K < 2$, the radicand in (9) eventually becomes negative at some t, which corresponds to the recollapse; all three situations are presented in Fig. 1. In black, we presented the $\kappa K < 2$ case. In dashed gray, we presented the $\kappa K = 2$ case, and in solid gray, we presented the $\kappa K > 2$ case.

Now let us turn to the $\Lambda \neq 0$ case. In that case, we can reduce the first of (8) to the biquadratic equation with respect to ρ and find the condition when its discriminant is negative; in that case, $\dot{\rho}^2 > 0$ always. This happens if

$$\Lambda \geq \Lambda_0 = \tfrac{3}{8} \tfrac{(\kappa K - 2)^2}{\lambda \kappa K}. \tag{11}$$

Now, let us plot the $\dot{\rho}(\rho)$ phase portrait; we did it for $\kappa K < 2$ in Fig. 2 for three cases: with the discriminant of (8) being positive (black curve), zeroth (solid gray), and negative (dashed gray). One can see that the only smooth and nonsingular regime occurs when the discriminant is negative so (11) is fulfilled. In the two other cases, one faces a finite-time future singularity at some finite t. So, to have a smooth and nonsingular regime for the $\kappa K < 2$ case, we need $\Lambda > \Lambda_0$ from (11). For the $\kappa K = 2$ case, as we can see from (11) that any $\Lambda > 0$ is sufficient; the $\kappa K > 2$ case is unaffected by (11).

The late-time regime in this case is described by the $\rho(t) \to \infty$ branch from Fig. 2. It could be derived from the first of (8) taking the mentioned limit. The dynamical equation reduces to $\dot{\rho}(t)^2 \simeq \Lambda \rho(t)^2/3$ with expanding solution $\rho(t) \propto \exp(\sqrt{\Lambda/3}t)$, which is the usual exponential solution.

Our claim that the $\kappa K > 2$ case is unaffected by (11) could be proved as follows: From the first of (8), one can see that for $\kappa K \geq 2$ we always have $\dot{\rho}^2 > 0$, given λ, Λ, $\kappa K > 0$. Of these, $\lambda > 0$ and $K > 0$ come from the Skyrme theory and $\kappa > 0$ since we have gravitational attraction. On the contrary, sometimes in different aspects of field theory $\Lambda < 0$ is considered, which gives anti-de Sitter in the cosmological background. One can immediately see from the first of (8) that in the $\Lambda < 0$ case at small ρ we have $\dot{\rho}^2 > 0$, while at large ρ it is negative. So the dynamics is limited, and we have a finite-time future singularity at some finite t, similar to the $\kappa K < 2$, $\Lambda < \Lambda_{cr}$ case. In the case of negative Λ, it is true regardless of κK, so in the remaining part of the paper, we consider $\Lambda > 0$ only.

To summarize our findings of the $a(t) \equiv 1$ case, if $\Lambda = 0$, there are three regimes, depending on the κK: If $\kappa K < 2$, there is a recollapse. If $\kappa K = 2$, the late-time regime is power-law $\rho(t) \propto \sqrt{t}$, and if $\kappa K > 2$, it is another power-law $\rho(t) \propto t$. If Λ is nonzero and negative, then we always have recollapse; if $\Lambda > 0$ and $\kappa K \geq 2$, we always reach the exponential regime $\rho(t) \propto \exp(\sqrt{\Lambda/3}t$. Finally, if $\Lambda > 0$ and $\kappa K < 2$, then if (11) is fulfilled, we have the exponential solution, and if not, we have recollapse. Let us note that all these regimes we derived analytically, and so

they should take place for all initial conditions. Our additional numerical analysis supports this claim.

IV. GENERAL CASE WITH DYNAMICAL $a(t)$

In this section, we analyze the behavior of the general system (7) with dynamical $a(t)$. First, we numerically analyze system (7) with $\Lambda = 0$ and present the typical behavior for each case in Figs. 3(a)–3(c). In panel (a), we present the typical behavior for the $\kappa K < 2$ case; one can see that it asymptotically tends to the $a(t) \equiv 1$ scenario with oscillations around it, and similar to the $a(t) \equiv 1$ counterpart, our dynamical $a(t)$ case has finite-time future singularity. In panel (b), we demonstrate typical $\kappa K = 2$ dynamics; one can see that, similar to the previous case, we have oscillations around the $a(t) \equiv 1$ regime with $\rho(t) \propto t^{1/2}$ asymptotic behavior. Finally, in panel (c), we present the $\kappa K > 2$ case with oscillations around $a(t) = 1$ and $\rho(t) \propto t$ asymptotic behavior. So we can see that in all $\Lambda = 0$ cases we have an oscillatory approach to the corresponding $a(t) \equiv 1$ cases, described in the previous section. Actual evolution curves depend on the initial conditions a bit (say, period and amplitude of oscillations depend on the initial conditions), but

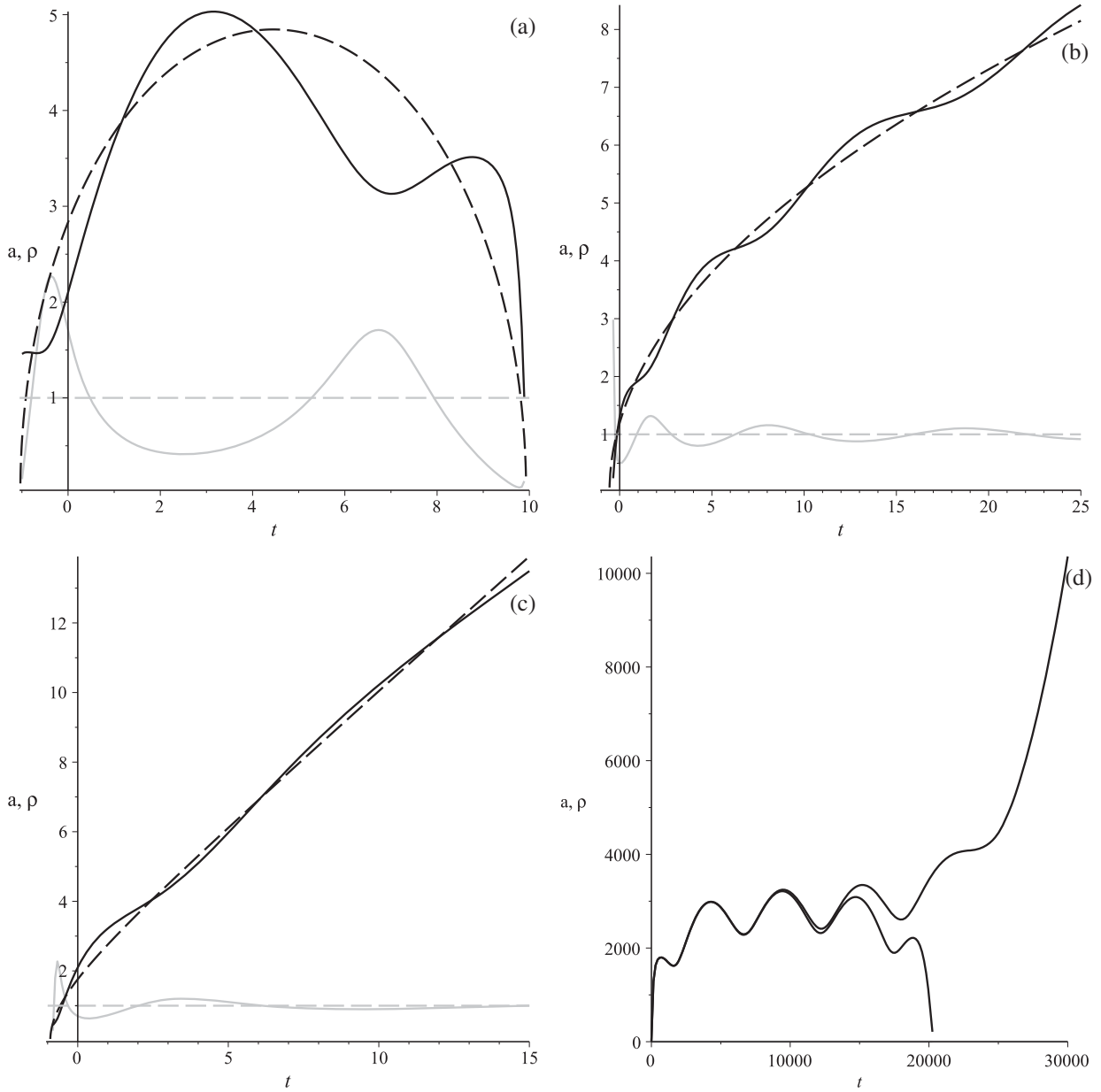

FIG. 3. Dynamics of $a(t) \neq 1$ and the $\Lambda = 0$ case on panels (a)–(c): $\kappa K < 2$ on panel (a), $\kappa K = 2$ on panel (b), and $\kappa K > 2$ on panel (c). On panel (d) is the dynamics of $a(t) \neq 1$ and the $\Lambda \neq 0$ case: exponential (upper curve) and recollapse (lower) behaviors (see the text for more details).

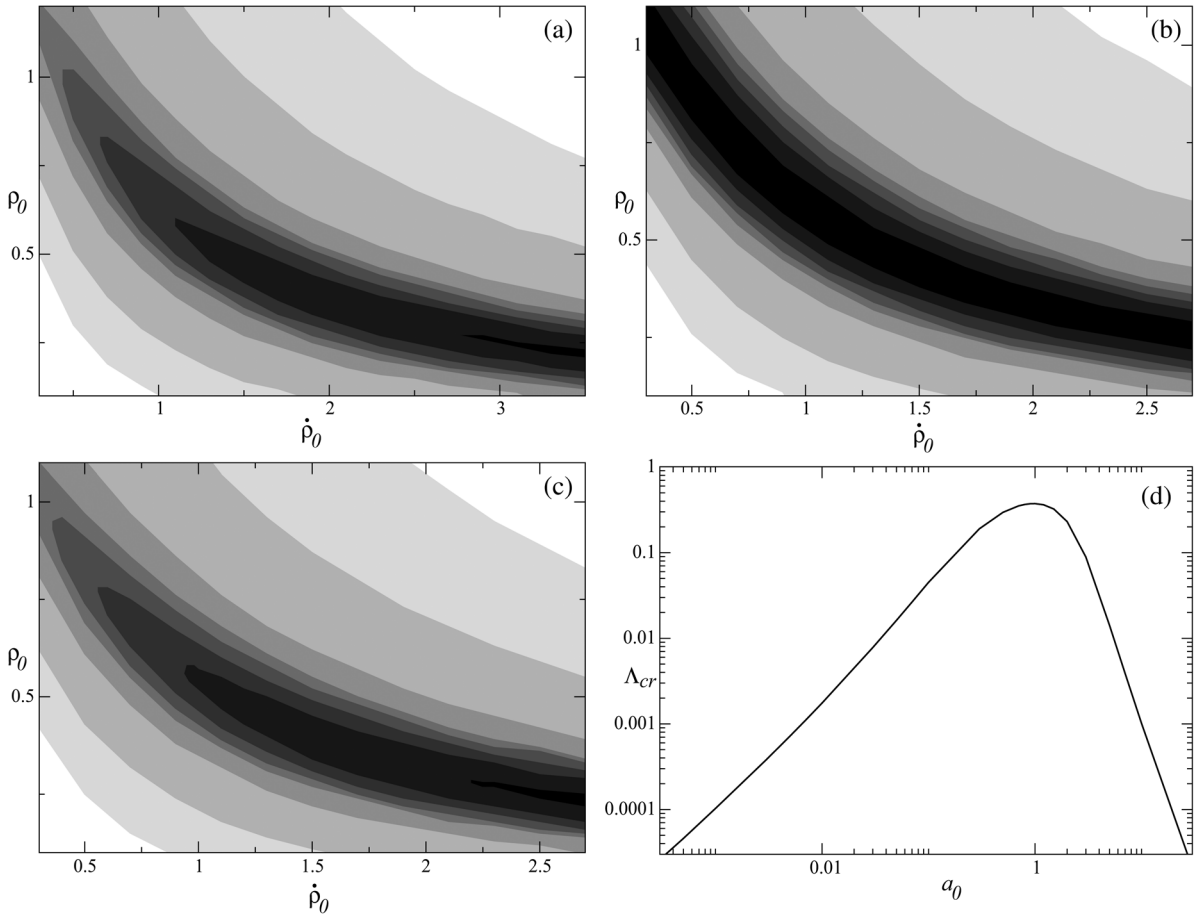

FIG. 4. Contours of equal Λ_{cr} on the initial conditions space $\{\rho_0, \dot{\rho}_0\}$ for $a_0 = 0.8$ on panel (a), $a_0 = 1.0$ on panel (b), and $a_0 = 1.2$ on panel (c). Example of Λ_{cr} behavior with varying a_0 on panel (d) (see the text for more details).

general behavior and late-time asymptotes are the same within the same case.

The final case to consider is general dynamical $a(t)$ with $\Lambda \neq 0$. As we just saw, with $\Lambda = 0$, dynamical $a(t)$ cases tend to their $a(t) \equiv 1$ counterparts through oscillation; the same behavior has dynamical $a(t)$ cases with nonzero Λ. So, similar to the $a(t) \equiv 1$ case, negative Λ always leads to recollapse regardless of κK. As we found in the previous section, $a(t) \equiv 1$ with $\Lambda > 0$ cases have either exponential regime or recollapse as a late-time attractor, and so dynamical $a(t)$ cases have the same attractor as well. For $\kappa K \geq 2$, we always have exponential solutions with damping oscillations, while for $\kappa K < 2$ we have either recollapse or exponential solution depending on Λ, which is the same behavior we described in the previous section for $a(t) \equiv 1$ case. In Fig. 3(d), we presented the typical behavior in the vicinity of separation of these two regimes. The lower regime experience recollapses, while the upper reaches exponential regime; both regimes experience oscillations.

In the general $\kappa K < 2$ case (with dynamical $a(t)$ with $\Lambda > 0$), the value for Λ_{cr}, which separates recollapse from exponential expansion [see this separation, e.g., in Fig. 3(d)], is actually lower then Λ_0, given by (11). Of course, generally $\Lambda_{cr} \leq \Lambda_0$, and actual values we present in Figs. 4(a)–4(c). We provided contours of equal Λ_{cr} on the initial conditions space $\{\rho_0, \dot{\rho}_0\}$ for $a_0 = 0.8$ on panel (a), $a_0 = 1.0$ on panel (b), and $a_0 = 1.2$ on panel (c). Levels correspond to 0.37, 0.36, 0.35, 0.34, 0.33, 0.3, 0.2, and 0.1 with decreasing blackness (so black is $\Lambda_{cr} \geq 0.37$, and white is $\Lambda_{cr} \leq 0.1$). As these contours are plot for $\lambda = 1$ and $\kappa K = 1$, which gives $\Lambda_0 = 0.375$ derived from (11), we can see that for $a_0 = 1$, presented in Fig. 4(b), Λ_0 is reached for all ρ_0 and $\dot{\rho}_0$ (so that for each ρ_0 exists $\dot{\rho}_0$ where Λ_0 is reached and vice versa). The utmost black corresponds to $\Lambda_{cr} \geq 0.37$. On the contrary, for a_0 different from 1, Λ_0 is reached for the lesser measure of the initial conditions, see Fig. 4(a) for $a_0 = 0.8$ and Fig. 4(c) for $a_0 = 1.2$. We can see from these two panels that Λ_0 is shifted towards higher $\dot{\rho}_0$, and with growth of the $|a_0 - 1|$ difference, the gap between the highest Λ_{cr} and Λ_0 also increase. In Fig. 4(d), we present a one-dimensional scan on a_0, and one can see that Λ_{cr} could be orders of magnitude below Λ_0.

Here is a short summary of this sections findings: We found that the $\Lambda = 0$ case with generic $a(t)$ has three distinct late-time regimes, which coincide with those

described in the previous $a(t) \equiv 1$ section. For $\kappa K < 2$, we have a recollapse. For $\kappa K = 2$, the late-time regime is power-law $\rho(t) \propto \sqrt{t}$, and for $\kappa K > 2$, it is another power-law $\rho(t) \propto t$. In the general $\Lambda > 0$ dynamical $a(t)$ case, again, similar to the $a(t) \equiv 1$ case, we have either an exponential solution or recollapse. The former of them takes place for $\kappa K \geq 2$, while the latter for $\kappa K < 2$ and $\Lambda < \Lambda_{cr}$. This $\Lambda_{cr} \leq \Lambda_0$ is defined from (11), and the actual value for Λ_{cr} heavily depends on the initial conditions, as presented in Fig. 4. One cannot miss the strong dependence of Λ_{cr} on a_0; with more initial anisotropy, a lesser value for the Λ-term is needed to reach exponential expansion.

V. LINEAR STABILITY

Now, let us turn our attention to the stability of the solutions. In the course of this paper, we saw there are three nonsingular regimes: two power-laws, $\rho(t) \propto \sqrt{t}$ and $\rho(t) \propto t$, and exponential $\rho(t) \propto \exp(Ht)$; all three regimes have $a(t) \to 1$. So, we perturb full system (7) around solution $a(t) = 1$ and with these three different $\rho(t)$. Linear perturbations around $a(t) = 1$ read $a \to 1 + \delta a$, $\dot{a} \to \dot{\delta a}$, $\ddot{a} \to \ddot{\delta a}$, $\rho \to \rho + \delta\rho$, $\dot{\rho} \to \dot{\rho} + \dot{\delta\rho}$, and $\ddot{\rho} \to \ddot{\rho} + \ddot{\delta\rho}$, and the equations on perturbations take the form

$$
\begin{aligned}
&4\rho^3\dot{\rho}\,\dot{\delta a} + 12\rho^2\dot{\rho}\,\dot{\delta\rho} + (-4\Lambda\rho^4 + 12\rho^2\dot{\rho} - 4\rho^2\kappa K + 8\rho^2 - 2\lambda\kappa K)\delta a + (-8\Lambda\rho^3 + 12\rho\dot{\rho} - 6\rho\kappa K + 12\rho)\delta\rho = 0,\\
&4\rho^3\ddot{\delta\rho} + 4\rho^2\dot{\rho}\,\dot{\delta\rho} + (-4\Lambda\rho^4 + 8\rho^3\ddot{\rho} + 4\rho^2\dot{\rho}^2 - 4\rho^2\kappa K - 8\rho^2 - 2\lambda\kappa K)\delta a + (-8\Lambda\rho^3 + 12\rho^2\ddot{\rho} + 4\rho\dot{\rho}^2 - 2\rho\kappa K + 4\rho)\delta\rho = 0,\\
&\rho^4\ddot{\delta a} + 3\rho^3\dot{\rho}\,\dot{\delta a} + (2\rho^2\kappa K + 8\rho^2 + 2\lambda\kappa K)\delta a = 0.
\end{aligned}
\tag{12}
$$

The last of (12) could be solved for stability in the a-direction. Substitution of exponential solution $\rho(t) = \rho_0 \exp(Ht)$ leads us to

$$
\rho_0^4 \exp(4Ht)(\ddot{\delta a}(t) + 3H\dot{\delta a}(t)) + 2\rho_0^2 \exp(2Ht)\delta a(t)(\kappa K + 4) + 2\kappa K\lambda\delta a(t) = 0. \tag{13}
$$

Using new variable $y = \dot{\delta a}(t)/\delta a(t)$, we can rewrite (13) as

$$
\begin{aligned}
&\dot{y} + y^2 + 3Hy + F(t) = 0,\\
&F(t) = \frac{2\kappa K}{\rho_0^2 e^{2Ht}} + \frac{8}{\rho_0^2 e^{2Ht}} + \frac{2\lambda\kappa K}{\rho_0^4 e^{4Ht}},
\end{aligned}
\tag{14}
$$

where $F(t)$ could be treated as a perturbative force acting on a system described by a homogeneous equation. The solution of the homogeneous equation from (14) is

$$
y(t) = \frac{3H}{3HC_1 e^{3Ht} - 1}, \tag{15}
$$

and then, we can solve it for $\delta a(t)$

$$
\delta a(t) = C_2(3HC_1 - e^{-3Ht}). \tag{16}
$$

The solution of the general equation (13) leads to an expression through M and W Whittaker functions [28] and generally cannot be expressed through elementary functions. But with an analysis performed in (14)–(16), we describe the general behavior as follows: $F(t)$ acts as a perturbative force and generates oscillations around (15), the solution of the homogeneous equation from (14). One can see that at $t \to \infty$, we have $F(t) \to 0$, so that at late times, we can use (15) as an exact solution, which leads to (16) as a solution for the original perturbation equation (13). One can note that the amplitude of perturbations does not damp to zero; as $t \to \infty$, we have $\delta a \to 3HC_1C_2$. The reason behind it is not clear, but as the perturbations do not grow, we treat this case as stable. Our numerical analysis totally supports this description. At the beginning, the solution is represented by damping oscillations, but after they decay, the asymptote value is not zero but some small constant. This is the same for a wide variety of the initial conditions, and the constant is also the same, though it varies for different parameters.

Now, let us turn our attention to the power-law regimes. In that case, the solution of the last of (12) could be written in terms of J and Y Bessel functions and is represented by oscillations with a damping amplitude, which directly points to stability, as long as solution itself exists. The solution for $\rho(t) = \rho_0\sqrt{t/t_0}$ exists iff $\rho_0^4 \geq 64\lambda t_0^2$, and the solution for $\rho(t) = \rho_0(t/t_0)$ exists iff $\rho_0^2 \geq 2(\kappa K + 4)$.

To summarize, we found that the exponential solution behave a bit unusually, but we claim that we could call it stable. The perturbations experience damping oscillations and reach constant value afterwards. As they do not grow, we claim them to be stable. The power-law solutions are stable everywhere within their range of existence.

VI. DISCUSSION

In the current paper, we considered the Bianchi-IX cosmological model in the Einstein-Skyrme system (7). The original system was simplified and considered with growth of complexity, which allows us to build a semi-analytical solution. Purely analytical solutions are obtained for the simplest case with $a(t) \equiv 1$ and $\Lambda = 0$ In that case,

there are three possible solutions: one with recollapse for $\kappa K < 2$ and two power-laws, $\propto t^{1/2}$ for $\kappa K = 2$ and $\propto t$ for $\kappa K > 2$. All three are presented in Fig. 1, and one cannot miss their similarity with three different Friedmann solutions from classical cosmology, with spatial curvature $k = \pm 1$ and 0. The scales with time are different, but the qualitative behavior is the same. In some sense, $(2 - \kappa K)$ plays a role similar to the spatial curvature.

Further complications of the system act as modifications of the obtained exact solution. Turning $a(t)$ dynamical (but still with $\Lambda = 0$) leads to oscillatory behavior like presented in Figs. 3(a)–3(c). Let us remind that oscillatory behavior is a part of the early Bianchi-IX universe, as discovered by Belinskij, Khalatnikov, and Lifshits [27]. If one keeps $a(t) \equiv 1$ but makes $\Lambda > 0$, then the power-law regimes turn exponential, while the recollapse regime turns to exponential if (11) is satisfied; if not, they remain recollapse. Finally, if one combines both dynamical $a(t)$ with $\Lambda > 0$, the resulting trajectories have oscillations and an exponential (de Sitter) late-time asymptote for $\kappa K \geq 2$. For $\kappa K < 2$, one has oscillations and de Sitter if $\Lambda > \Lambda_{cr}$ and recollapse if $\Lambda < \Lambda_{cr}$. The separation between these two cases is presented in Fig. 3(d). Recollapse behavior is also encountered in the anti-de Sitter case, when $\Lambda < 0$, and in this case, the result is independent on κK. The value for Λ_{cr} cannot exceed Λ_0 from (11) but could be much less (orders of magnitude), as our numerical investigation suggests. In Fig. 4, we provided the distribution of Λ_{cr} over initial conditions space for three different a_0 on panels (a)–(c) and a linear cut over a_0 on panel (d).

One can see that all nonsingular regimes have $a(t) \to 1$ at late times. From the metric (5) point of view, the $a(t) = 1$ solution is the most symmetric one (so that it has more Killing fields then $a(t) \neq 1$ one). We can see that all nonsingular regimes have symmetry restoring dynamics, and all these solutions are stable. Singular regimes, which do not possess this feature, are either $\kappa K < 2$ cases with $\Lambda < \Lambda_{cr}$ or $\Lambda < 0$ AdS cases; for the latter, the value for κK is irrelevant.

For more physical analysis, we use real values for the Skyrme coupling constants [29]. Then, one can immediately see that $\kappa K \lll 1$, and so $\kappa K < 2$ is the case. For $\kappa K < 2$ from (9), one can derive the "lifetime," with real values for couplings substituted, this time appears to be of the order of Planck time, which means that without the Λ-term or some other matter sources with sufficient density the Bianchi-IX universe with Skyrme would collapse immediately. On the other hand, on this time scale, space-time cannot be described by classical means, and additional investigation with involvement of quantum physics is required. Finally, if we substitute coupling constants into (11), the resulting value for the cosmological constant appears to be in agreement with other estimates from quantum field theory, treating it as vacuum energy, and is around 120 orders of magnitude higher than the observed value (so-called "cosmological constant problem", see, e.g., [30]).

In a sense, the results of the current paper complement the results of [22], where we studied Bianchi-I and Kantowski-Sachs universes in the Einstein-Skyrme system. In both papers, the cosmological constant (or probably some other matter field) is necessary for viable cosmological behavior. But unlike [22], where we demonstrated a need for the upper bound on the value of *the* Λ-term, in the current paper, we found the lower bound. It is interesting that different topologies in the presence of the Skyrme source require either not too large or not too low values for the cosmological constant.

This finalizes our study of the Bianchi-IX Skyrme-Einstein system. We described its dynamics and derived conditions for different regimes to take place. Generally, Einstein-Skyrme systems are very interesting and are not much considered, probably due to their complexity, so each new result improves our understanding of cosmological hadron dynamics. In particular, these systems offer the interesting possibility to study the cosmological consequences to have conserved topological charge. Thus, the present analysis is quite relevant as the energy-momentum tensor is a Skyrmions of unit topological charge.

ACKNOWLEDGMENTS

This work was supported by FAPEMA under Project No. BPV-00038/16. We are thankful to the referee for their valuable comments which lead to improving the manuscript.

[1] N. Manton and P. Sutcliffe, *Topological Solitons* (Cambridge University Press, Cambridge, 2007).
[2] T. Skyrme, Proc. R. Soc. A **260**, 127 (1961); **262**, 237 (1961); Nucl. Phys. **31**, 556 (1962).
[3] *Duality and Supersymmetric Theories*, edited by D. I. Olive and P. C. West (Cambridge University Press, Cambridge, 1999).
[4] A. P. Balachandran, H. Gomm, and R. D. Sorkin, Nucl. Phys. **B281**, 573 (1987).
[5] A. P. Balachandran, A. Barducci, F. Lizzi, V. G. J. Rodgers, and A. Stern, Phys. Rev. Lett. **52**, 887 (1984).
[6] A. P. Balachandran, F. Lizzi, V. G. J. Rodgers, and A. Stern, Nucl. Phys. **B256**, 525 (1985).

[7] G. S. Adkins, C. R. Nappi, and E. Witten, Nucl. Phys. **B228**, 552 (1983).
[8] E. Guadagnini, Nucl. Phys. **B236**, 35 (1984).
[9] E. Witten, Nucl. Phys. **B223**, 422 (1983); **B223**, 433 (1983).
[10] H. Pais and J. R. Stone, Phys. Rev. Lett. **109**, 151101 (2012).
[11] U. Al Khawaja and H. Stoof, Nature (London) **411**, 918 (2001).
[12] J.-I. Fukuda and S. Zumer, Nat. Commun. **2**, 246 (2011).
[13] S. Mühlbauer, B. Binz, F. Jonietz, C. Pfleiderer, A. Rosch, A. Neubauer, R. Georgii, and P. Böni, Science **323**, 915 (2009).
[14] A. N. Bogdanov and D. A. Yablonsky, Sov. Phys. J. Exp Theor. Phys. **68**, 101 (1989).
[15] T. Sakai and S. Sugimoto, Prog. Theor. Phys. **113**, 843 (2005).
[16] F. Canfora and P. Salgado-Rebolledo, Phys. Rev. D **87**, 045023 (2013); F. Canfora and H. Maeda, Phys. Rev. D **87**, 084049 (2013).
[17] H. Luckock and I. Moss, Phys. Lett. B **176**, 341 (1986); S. Droz, M. Heusler, and N. Straumann, Phys. Lett. B **268**, 371 (1991).
[18] S. Droz, M. Heusler, and N. Straumann, Phys. Lett. B **271**, 61 (1991).
[19] N. K. Glendenning, T. Kodama, and F. R. Klinkhamer, Phys. Rev. D **38**, 3226 (1988); B. M. A. G. Piette and G. I. Probert, Phys. Rev. D **75**, 125023 (2007); G. W. Gibbons, C. M. Warnick, and W. W. Wong, J. Math. Phys. (N.Y.) **52**, 012905 (2011); S. Nelmes and B. M. A. G. Piette, Phys. Rev. D **84**, 085017 (2011).
[20] P. Bizon and T. Chmaj, Phys. Rev. D **58**, 041501 (1998); P. Bizon, T. Chmaj, and A. Rostworowski, Phys. Rev. D **75**, 121702 (2007); S. Zajac, Acta Phys. Pol. B **40**, 1617 (2009); **42**, 249 (2011).
[21] N. Sawado, N. Shiiki, K.-i. Maeda, and T. Torii, Gen. Relativ. Gravit. **36**, 1361 (2004); H. Sato, N. Sawado, and N. Shiiki, Phys. Rev. D **75**, 014011 (2007); T. Ioannidou, B. Kleihaus, and W. Zakrzewski, Phys. Lett. B **600**, 116 (2004); **643**, 213 (2006); **635**, 161 (2006); H. Sato and N. Sawado, Phys. Lett. B **660**, 72 (2008).
[22] F. Canfora, A. Giacomini, and S. A. Pavluchenko, Phys. Rev. D **90**, 043516 (2014).
[23] L. Parisi, N. Radicella, and G. Vilasi, Phys. Rev. D **91**, 063533 (2015).
[24] E. Ayon-Beato, F. Canfora, and J. Zanelli, Phys. Lett. B **752**, 201 (2016).
[25] F. Canfora, Phys. Rev. D **88**, 065028 (2013); F. Canfora, F. Correa, and J. Zanelli, Phys. Rev. D **90**, 085002 (2014).
[26] F. Canfora, M. D. Mauro, M. A. Kurkov, and A. Naddeo, Eur. Phys. J. C **75**, 443 (2015).
[27] V. A. Belinskij, I. M. Khalatnikov, and E. M. Lifshits, Adv. Phys. **19**, 525 (1970); **31**, 639 (1982).
[28] M. Abramowitz and I. Stegun, *Handbook of Mathematical Functions* (Dover Publications, New York, 1972); Y. Luke, *The Special Functions and Their Approximations* (Academic Press, New York, 1969), Vol. 1.
[29] G. S. Adkins, C. R. Nappi, and E. Witten, Nucl. Phys. **B228**, 552 (1983).
[30] S. Weinberg, Rev. Mod. Phys. **61**, 1 (1989).